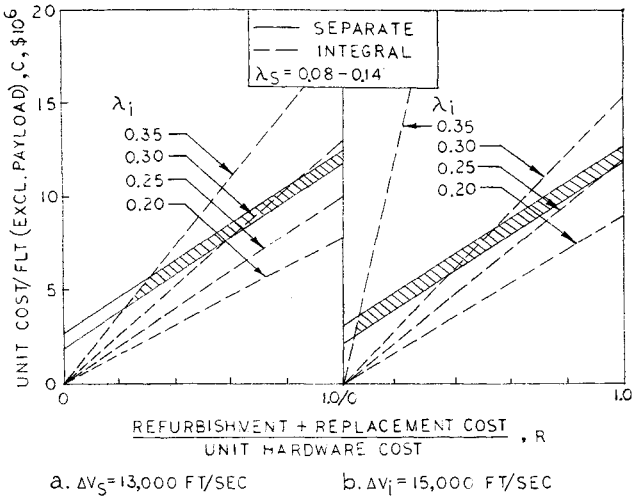

Fig. 2 Unit cost per flight vs refurbishment-replacement factor ($I_s = I_i = 450$ sec).

their gross weights are about equal, which as shown later they are, for many cases of interest). Both separate and integral concepts can therefore be assumed to have equivalent preceding stages, whether they be of recoverable, expendable, drop tank or other variety.

Performance Comparison

The performance of the two vehicle concepts can be described using the ideal rocket equation.

$$\Delta v_s = gI_s \ln[(w_p + w_s)/(w_p + \lambda w_s)] \quad (1)$$

$$\Delta v_i = gI_i \ln[(w_u + w_i)/(w_u + \lambda w_i)] \quad (1a)$$

Since the gross weights of the vehicles are $w_{gs} = w_p + w_s$ and $w_{gi} = w_u + w_i$, it can be shown by substitution in Eqs. (1) and (1a) that

$$w_{gs} = w_p(\lambda_s - 1)e^{\Delta v_s/gI_s}/(\lambda_s e^{\Delta v_s/gI_s} - 1) \quad (2)$$

$$w_{gi} = w_u(\lambda_i - 1)e^{\Delta v_i/gI_i}/(\lambda_i e^{\Delta v_i/gI_i} - 1) \quad (2a)$$

Equations (2) and (2a) are plotted in Fig. 1 for various values of Δv and λ, and for $I_s = I_i = 450$ sec to represent high-pressure hydrogen-oxygen propulsion. Typical regions of interest are shown by the shaded areas. The most prominent indication of Fig. 2 is the strong sensitivity of the integral concept, to uncertainties in structure factor λ_i. If $\lambda_i <$ about 0.3 can be achieved, the integral concept is competitive with or preferable to the separate concept on a gross weight basis; but if λ_i much exceeds the vicinity of 0.3, then the integral concept quickly becomes not only relatively heavy, but progressively even more sensitive to λ_i.

Cost Comparison

The flight hardware cost per flight for the two vehicles can be written

$$C_{p+s} = c_p R + c_s \quad (3)$$

$$C_i = c_i R \quad (4)$$

where c_p does not include useful payload cost and neither c_s nor c_i include propellant costs, which in any case are negligible compared to hardware costs.

The hardware costs were developed using cost estimating relationships involving materials cost and manufacturing hours per pound, air frame dry weight, and expended propellant weight for the expendable stage, and involving historical and point design vehicle costs and manufactured hardware weight of ablative and radiative manned spacecraft for the reusable vehicles. Using these estimated costs, Eqs. (3) and (4) are plotted in Fig. 2a and 2b for ideal velocity gains of 13,000 and 15,000 fps, respectively. Because of the uncertainties associated with them, structure factors and refurbishment-replacement factors are varied parametrically.

These results indicate that if a λ_i of 0.25 can be achieved, then the integral spacecraft is more economical in essentially all cases considered. If $\lambda_i = 0.30$, the integral concept is more economical for values of R less than 39 to 84%. Even if λ_i is as high as 0.35, the integral concept is more economical for values of R less than 15 to 32%.

Observations

1) Integral spacecraft are indicated to be competitive with, or preferable to, separate spacecraft in both cost and gross weight for a considerable range of structure factors and refurbishment-replacement factors, for velocity gains of 13,000 to 15,000 fps. At lower velocity gains, separate spacecraft may be at a greater advantage because of structure factor penalties to the integral concept which result inevitably from smaller vehicle sizes, and from the fixed structural weights needed to enclose and carry the payload. At higher velocity gains, integral spacecraft probably have the advantage because of the more favorable structure factors accompanying larger sizes.

2) Because of the performance sensitivity of the integral concept to structural dead weight, it appears mandatory that the structure factor as defined here be held to the vicinity of 0.30 or less. This emphasizes the importance of improvements in the technologies of high volumetric efficiency lifting bodies and lightweight structures and radiative thermal shields.

3) Aside from cost and performance advantages, integral manned spacecraft appear to offer increased reliability by eliminating staging and increased flexibility from more favorable cross range, landing characteristics and refurbishment (all by virtue of decreased planform loading during and after entry).

4) Although integral spacecraft may involve somewhat higher research and development costs than separate concepts, and their characteristics are more sensitive to structure factor, their potential advantages appear to render integral spacecraft concepts worthy of increased interest and study.

Effects of Oblique Shock Waves in the Near Field of Rocket Plumes

JARVIS LENG,* CHARLES W. OSONITSCH,† AND THOMAS M. LACINSKI‡
Grumman Aerospace Corporation, Bethpage, N. Y.

IN Ref. 1 we described a technique for laboratory simulation of rocket plumes in space. Some sample results showed that stagnation-point heating along the thrust axis was higher

Received July 22, 1969; revision received August 19, 1969. The experimental data presented herein were obtained in the course of development work at Grumman on the Apollo Project Lunar Module, supported by NASA Contract NAS 9-1100, and the Apollo Applications Program LM-A, supported by NASA Contract NAS 8-25000. The authors would like to thank the many members of the Grumman Research Fluid Mechanics Section who helped in the interpretation of these flowfields.

* Research Engineer, Research Department. Member AIAA.
† Thermal Control Engineer, LM Thermodynamics Section. Member AIAA.
‡ Research Engineer, Research Department.

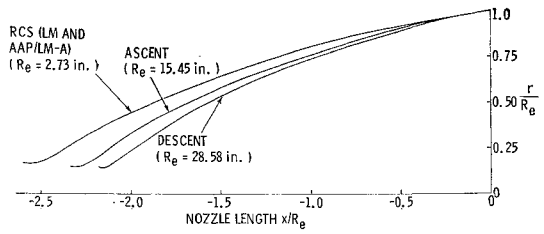

Fig. 1 Contours of LM ascent, descent, and RCS engine nozzles.

than predicted by characteristics theory in the near field. Also, photographs of flow luminosity resulting from impingement of the plumes on surfaces normal to the thrust axis showed considerable complexity in the flowfields. This Note presents additional data that indicate that these phenomena can be explained by the presence of oblique shock waves originating within the nozzle. Such waves are generated in nozzles when, after rapid expansion near the throat, the flow is turned back toward the centerline by an inflection in the wall contour. Other investigators have noted such waves in both contoured[2] and conical[3] nozzles, but, generally speaking, their effects in plume impingement problems have not been considered (see, e.g., Refs. 4–9). Neglect of such nonuniformities at the nozzle exit plane may lead to poor predictions in the near field, which is important to the design of plume deflectors, spacecraft thermal shielding, and problems associated with retro-rocket landings and staging. One analytical technique for describing plumes containing oblique shock waves is given by Rochelle.[10]

Discussion of Experiments

The experimental data presented herein were obtained in our short-duration, detonation-tube facility[1] at combustion chamber to ambient background pressure ratios between 10^8 and 10^9, simulating scaled-down rocket engines run at full-scale Reynolds number, enthalpy, and chemical element balance. The background pressure was $\approx 10^{-5}$ torr, adequately representing the hard vacuum of space, where no plume boundary effects are present.The scaled rocket engines represented the Apollo Lunar Module (LM) ascent, descent, and reaction control system (RCS) engines, and the Apollo Applications Program (AAP)/LM-A RCS engines. These four engines have almost identical combustion chamber properties and similar nozzle contours (Fig. 1) but are substantially different in size. As can be seen from Fig. 1, the origin of the axial coordinate x is at the nozzle exit plane. All coordinates are nondimensionalized with respect to the nozzle exit radius, R_e.

Data from a $\frac{1}{20}$-scale LM descent nozzle exhaust impinging on a flat plate perpendicular to the nozzle centerline were obtained for several nozzle exit plane-to-surface separation distances S. The stagnation chamber properties simulated the full-scale engine running at the nominal "hovering" thrust level of 25% full throttle. For $S/R_e < 0.5$, nozzle wall static pressure measurements[11] indicate the presence of a shock wave extending across the nozzle. Figure 2a is a schlieren photograph showing a flowfield typical of those for $S/R_e < 0.5$. At $S/R_e = 0.5$ the peripheral area at the lip between the nozzle exit plane and the flat plate becomes equal to the nozzle exit area, and, at $S/R_e = 0.56$, the nozzle wall static pressure measurements no longer indicate a shock wave extending to the nozzle wall. (A similar result for the LM RCS engine was reported.[12]) For $S/R_e = 0.56$, however, a conical, oblique shock wave extends from within the nozzle to the downstream surface (Fig. 2b). At $S/R_e \approx 1.0$ the oblique shock wave extending to the plate is bounded across the top by a normal shock, giving the appearance of a cone frustum (Fig. 2c). At $S/R_e \approx 3.5$ the cone frustum shock pattern is no longer present, and only the anticipated concave dish-shaped shock wave is seen (Fig. 2d). There

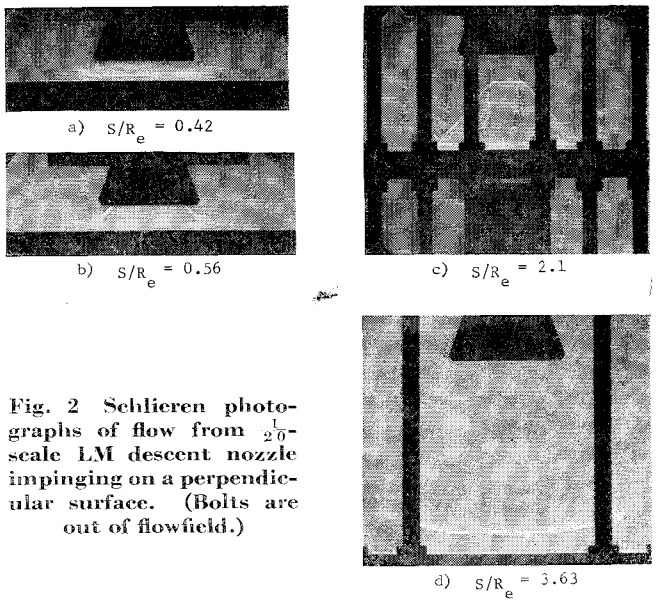

Fig. 2 Schlieren photographs of flow from $\frac{1}{20}$-scale LM descent nozzle impinging on a perpendicular surface. (Bolts are out of flowfield.)

are no further basic changes in the flowfield shock patterns for $S/R_e > 3.5$. For all $S/R_e > 0.56$ the nozzle lip expansion wave is visible in the schlieren photographs, indicating that the nozzle flow is fully developed and supersonic.

These schlieren photographs and pressure measurements lead us to believe that another shock wave comes from within the nozzle and joins the plate wave at the point where the latter is terminated by the normal shock (Fig. 3). This additional wave is too weak to be sensed by our schlieren system, but it must be present for the cone frustum pattern (Fig. 2c) to exist. The situation is analogous to the barrel-shock, normal-shock (Mach disk) system that occurs when an underexpanded, supersonic jet exhausts into a finite back pressure environment.[13,14] In the descent engine case the shock system results from the physical boundaries of the nozzle and the flat plate rather than from the background pressure of the ambient gas. Because of the high-vacuum background in our tests there is no subsonic path connecting the plate to the nozzle for all $S/R_e > 0.56$. The position of the nozzle oblique shock wave, therefore, is unaltered as the plate is moved; only the point of intersection of the nozzle and plate waves is changed.

Snedeker and Donaldson have shown[13] that in the presence of a Mach disk a reverse flow region (separation bubble) can exist around the centerline on a perpendicular impingement surface. The sketches in Fig. 3 include such separation bubbles, but our surface pressure measurements were not sufficiently fine to say with certainty that such bubbles were present.

Although we could not see the nozzle oblique wave, its location could be inferred from the series of schlieren pictures for $0.56 < S/R_e < 3.5$. Figure 4 shows the positions of the conical frustum shock patterns for various S's and the inferred nozzle oblique shock wave. By extrapolating the nozzle oblique shock wave, we found that it would cross

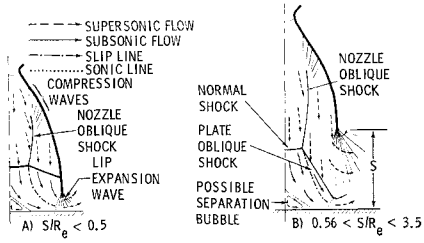

Fig. 3 Essential features of nozzle flow impingement on perpendicular surface for $S/R_e < \sim 3.5$. (Not to scale.)

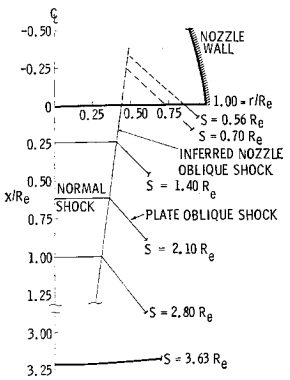

Fig. 4 Location of LM descent nozzle shock wave system as deduced from schlieren photographs of flow impingement on perpendicular surface for six different separation distances S.

the axis at $S \approx 3.5\ R_e$, which corresponds to the S at which the flow pattern changes from that shown in Fig. 2c to that shown in Fig. 2d.

Flat-plate surface-pressure distributions were also obtained,[15] and representative centerline values for various S's are shown in Fig. 5. Coincident with the change in flow pattern from the cone frustum shock system to the dish-shaped shock is an increase in surface pressure when S/R_e is increased from 2.8 to ~3.5. Similar results were reported in Ref. 2. We believe that this rise occurs because the nozzle oblique wave crosses the axis at $S/R_e \simeq 3.5$, and the pressure recovered through this oblique shock wave and then a normal shock wave exceeds that obtained through the normal shock alone at smaller S's. Thus, for a small range of S's just beyond 3.5 R_e, the stagnation pressure increases. For larger S's, the normal-shock pressure losses increase, and the stagnation pressure again decreases.[2]

One point of concern is whether the flowfields generated during a lunar landing are properly simulated by tests with fixed model-to-surface positions. The starting process of a nozzle close to a surface could result in a stable flow pattern different from that of a fully started nozzle being brought slowly down to the same position. We cannot answer the question irrefutably, but, because there are no plume boundary effects present in either the actual lunar landing or the detonation-tube experiments, and because the flow passages downstream of the nozzle exit are sufficiently large, we believe that the simulation is valid. Of course, the dynamics of cratering (soil erosion) and surface particle entrainment cannot be simulated by this kind of test.

Evidence that the LM ascent engine produces flowfields almost identical to those for the descent engine is given by self-luminosity photographs[1] of $\frac{1}{10}$-scale, "fire-in-the-hole" staging tests. These pictures[1] show patterns of incandescent gas very similar to the shock wave patterns seen in Fig. 2, because the shock waves heat the gas that flows through them, and certain species present radiate in the visible region at the resulting temperatures.

Figures 6 shows schlieren photographs of the plume from a $\frac{1}{4}$-scale LM RCS nozzle impinging on a normal, flat surface. The flow patterns are qualitatively and quantitatively similar to those in Fig. 2, except that the shock wave structure on the plate is more rounded. This would come about if the central core flow from the RCS engine were more nonuniform than that from the ascent and descent engines. Examples of nonuniform core flows may be found in the schlieren photographs of Ref. 2 and the shadowgraphs of Ref. 14.

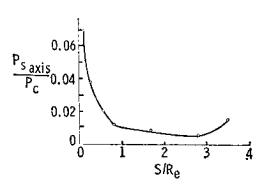

Fig. 5 Surface pressures produced on a flat plate at the nozzle axis point; $\frac{1}{20}$-scale LM descent engine running at 25% thrust.[15]

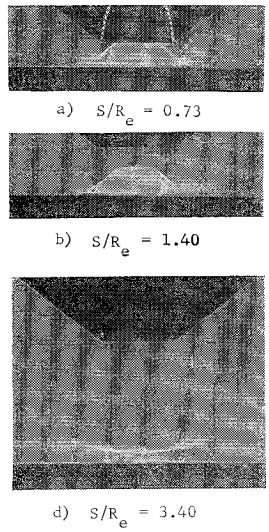

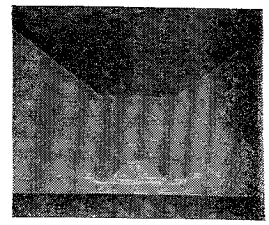

Fig. 6 Schlieren photographs of flow from $\frac{1}{4}$-scale LM RCS nozzle impinging on a perpendicular surface.

Supporting evidence for nozzle oblique shocks appears to be provided by heat-transfer measurements[16,17] on plume deflectors. The deflectors, proposed for both the LM and the AAP/LM-A vehicles, are curved surfaces developed from conic sections, and are placed under the RCS engines to protect nearby spacecraft surfaces from direct plume impingement. Surface pressures on, and heat-transfer rates to, these deflectors from $\frac{1}{4}$-scale LM and AAP/LM-A RCS engines were measured. The engines have identical nozzle contours (Fig. 1), but operate with slightly different fuels. A typical surface heat-transfer rate ($\dot{q}$) distribution along the centerline of the AAP/LM-A plume deflector, set at an angle of 22° to the nozzle centerline, is shown in Fig. 7. The significant point is the second peak in this $\dot{q}$ distribution. This peak is believed to correspond to the point of impingement of the nozzle oblique shock wave on the deflector.

Figure 8 shows a sketch of the flow along the plume deflector centerline and also the experimentally determined locus of the second $\dot{q}$ peaks for different positions of the deflector. This locus is assumed to correspond to the path of the oblique shock after it has crossed the axis of the nozzle. The point where it crosses the axis was obtained by noting the S/R_e (~3.3) at which the flowfield changes from that of Fig. 6c to that of Fig. 6d. High-speed, self-luminosity motion pictures, looking at the planform of the plume deflector, showed that an elliptical bright spot always occurred in the region of the second $\dot{q}$ peak. Also shown in Fig. 8 is the oblique-shock-wave pattern predicted by Rochelle[10] for a flow with our oxidizer/fuel ratio (2.0), assuming frozen flow from the nozzle throat. His method is the only one known to us to provide a correct qualitative picture of the near-field plume; however, the predicted location of the oblique shock wave is well upstream of that inferred from our measurements.

Concluding Remarks

Oblique shock waves are believed to exist in all of the four contoured rocket nozzles that we tested. The impingement of these oblique waves on adjacent spacecraft components and nearby surfaces can radically affect flowfields, heat transfer, and pressure distributions. Therefore, we recommend that analytical predictions of near-field plume impingement flows take into account such waves. Analyses valid

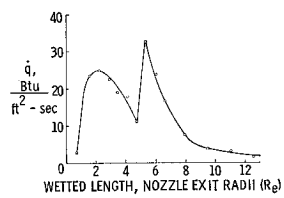

Fig. 7 Distribution of heat-transfer rate along the centerline of a plume deflector canted at 22° with respect to the nozzle axis.[17]

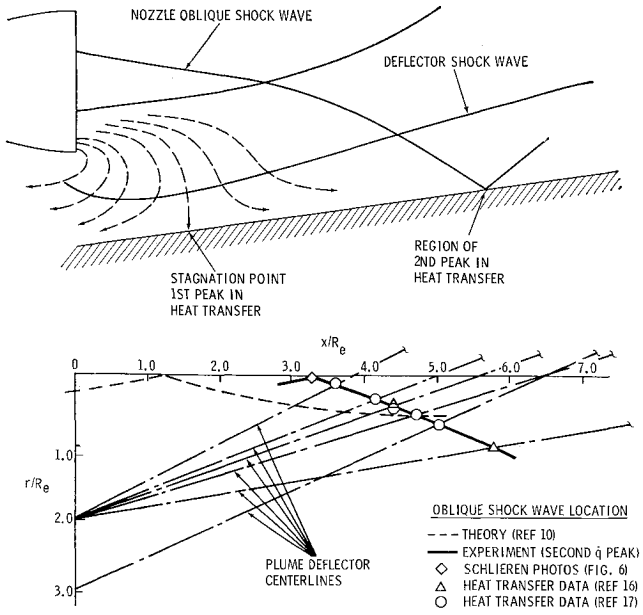

Fig. 8 Sketch of flow along plume deflector centerline and scale drawing of nozzle oblique shock wave location inferred from second $\dot{q}$ peaks on plume deflector centerlines ($\frac{1}{4}$-scale LM RCS nozzle).

in the far field may give very misleading results when applied to near-field problems.

References

[1] Leng, J., Oman, R. A., and Hopkins, H. B., "A Detonation Tube Technique for Simulating Rocket Plumes in a Space Environment," *Journal of Spacecraft and Rockets*, Vol. 5, No. 10, Oct. 1968, pp. 1148–1154.

[2] Stitt, L. E. and Latto, W. T., "Highly Underexpanded Exhaust Jets Against Adjacent Surfaces," *Astronautics and Aerospace Engineering*, Vol. 1, No. 1, Feb. 1963, pp. 107–110.

[3] Back, L. H. and Cuffel, R. F., "Detection of Oblique Shocks in a Conical Nozzle with a Circular-Arc Throat," *AIAA Journal*, Vol. 4, No. 12, Dec. 1966, pp. 2219–2221.

[4] Eastman, D. W. and Radtke, L. P., "Flow Field of an Exhaust Plume Impinging on a Simulated Lunar Surface," *AIAA Journal*, Vol. 1, No. 6, June 1963, pp. 1430–1431.

[5] Andrews, E. H., Vick, A. R., and Craidon, C. B., "Theoretical Boundaries and Internal Characteristics of Exhaust Plumes from Three Different Supersonic Nozzles," TN D-2650, March 1965, NASA.

[6] Roberts, L., "The Interaction of a Rocket Exhaust with the Lunar Surface," *The Fluid Dynamic Aspects of Space Flight*, AGARDograph 87, Vol. 2, Gordon and Breach, New York, 1966, pp. 269–290.

[7] Piesik, E. T., Koppang, R. R., and Simkin, D. J., "Rocket-Exhaust Impingement on a Flat Plate at High Vacuum," *Journal of Spacecraft and Rockets*, Vol. 3, No. 11, Nov. 1966, pp. 1650–1657.

[8] Herron, R. D., "Jet-Boundary Simulation Parameters for Underexpanded Jets in a Quiescent Atmosphere," *Journal of Spacecraft and Rockets*, Vol. 5, No. 10, Oct. 1968, pp. 1155–1160.

[9] Brook, J. W., "Far Field Approximation for a Nozzle Exhausting into a Vacuum," *Journal of Spacecraft and Rockets*, Vol. 6, No. 5, May 1969, pp. 626–628.

[10] Rochelle, W. C., *LM RCS Plume Impingement Study*, Rept. 68.3352.16–26, Dec. 1968, TRW Systems, Redondo Beach, Calif.

[11] Nelson, T., Rice, R., and Rosenstock, J., *Results of the First Series of $\frac{1}{20}$-Scale Shock Tube Fire-Till-Touchdown Tests*, LM Engineering Memo LMO-510-984, Oct. 1968, Grumman Aerospace Corp., Bethpage, N.Y.

[12] Clark, L. V., *LM Base Pressures and Retro Nozzle Choking During Simulated Lunar Touchdown*, LWP-632, July 1968, NASA.

[13] Snedeker, R. S. and Donaldson, C. duP., *Experiments on Free and Impinging Underexpanded Jets from a Convergent Nozzle*, Rept. 63, Sept. 1964, Aeronautical Research Associates of Princeton.

[14] Adamson, T. C., Jr. and Nicholls, J. A., "On the Structure of Jets from Highly Underexpanded Nozzles Into Still Air," *Journal of the Aerospace Sciences*, Vol. 26, No. 1, Jan. 1959, pp. 16–24.

[15] Rosenstock, J., Nelson, T., and Rice, R., *Results of the Third Series of $\frac{1}{20}$-Scale Shock Tube Fire-Till-Touchdown Tests*, LM Engineering Memo LMO-510-1093, Feb. 1969, Grumman Aerospace Corp., Bethpage, N.Y.

[16] Osonitsch, C., *Analysis of Shock Tunnel RCS Plume Deflector Pressure and Heat Transfer Data*, LM Engineering Memo LMO-510-1060, Jan. 1969, Grumman Aerospace Corp., Bethpage, N.Y.

[17] Mendelsohn, A. R. and Holland, C., *The LM-A Plume Deflector Aerothermodynamics Analysis and Shock Tunnel Test*, AAP/LM-A Rept. ARP251-6, March 1969, Grumman Aerospace Corp., Bethpage, N.Y.

Projectile Size and Density Effects on Hypervelocity Penetration

R. J. Arenz, S.J.*

Loyola University of Los Angeles, Los Angeles, Calif.

Nomenclature

D = diameter of hole in shield or first sheet, in.
d = diameter of projectile, in.
P = depth of penetration of single target sheet, in.
P_T = total depth of penetration of shield and backup sheet, in.
S = sheet spacing, in.
t = thickness of sheet, in.; t_b for backup sheet; t_s for shield or first sheet; t_∞ for single sheet required for quasi-infinite response
t_T* = "ballistic limit" = value of $(t_s + t_b)/d$ to resist mechanical failure on the inner surface
V = velocity of impact, km/sec
ρ = density of projectile material, g/cm^3

Introduction

THE current generation of spacecraft has incorporated meteoroid shielding appropriate for relatively short-term near-earth and cislunar missions. As planning turns to long duration space stations and interplanetary vehicles, designs must take into account the larger particles expected to be encountered on such extended missions and approaches to the asteroid belt. The NASA Manned Spacecraft Center recently sponsored an experimental test program at the light gas gun facility of the Douglas Aerophysics Laboratory.[1] It examined the penetration characteristics against dual-sheet structures of both low-density syntactic foam and aluminum spheres varying in diameter from 0.125 to 1.22 in. These results have been augmented with data from small aluminum projectiles fired at the NASA/MSC Meteroid Simulation Laboratory, and the scaling effects from both test series are reported here.

Presented as Paper 69-376 at the AIAA Hypervelocity Impact Conference, Cincinnati, Ohio, April 30–May 2, 1969; submitted April 30, 1969; revision received August 27, 1969. This work was sponsored by the NASA Manned Spacecraft Center, Houston, Texas, under a NASA-ASEE Summer Faculty Research Fellowship. It is a pleasure to acknowledge the suggestion of this research by B. G. Cour-Palais as well as helpful discussions with him and W. E. McAllum at the Manned Spacecraft Center.

* Assistant Professor, Department of Mechanical Engineering. Member AIAA.